

Optimizing a Biocatalyst for Improved NAD(P)H Regeneration: Directed Evolution of Phosphite Dehydrogenase

Ryan Woodyer[†], Wilfred A. van der Donk^{*,†} and Huimin Zhao^{*,†,‡}

Departments of Chemistry[†] and Chemical and Biomolecular Engineering[‡], University of Illinois at Urbana-Champaign, 600 S. Mathews Ave, Urbana, IL 61801, USA

Abstract: Cofactor regeneration is an important solution to the problem of implementing complex cofactor requiring enzymatic reactions at the industrial scale. NAD(P)H-dependent oxidoreductases are highly valuable biocatalysts, but the high cost of the pyridine cofactors necessitates *in situ* cofactor regeneration for preparative applications. Here we report the use of directed evolution to enhance the industrially important properties of phosphite dehydrogenase for NAD(P)H regeneration. A two-tiered sorting method of selection and screening was used in conjunction with random and rational mutagenesis. Following six rounds of directed evolution, soluble expression in *E. coli* was increased more than 3-fold, while the turnover rate was increased about 2-fold, effectively lowering the cost of the enzyme by >6-fold. Large-scale production of the final mutant enzyme by fermentation resulted in ~6-times higher yield (Units/Liter) than the WT enzyme. The enhancements of PTDH were independent of expression vector and *E. coli* strain utilized. The advantage of the final mutant over the WT enzyme was demonstrated using the industrially relevant bioconversion of trimethylpyruvate to *L-tert*-leucine. The mutations discovered are discussed in the context of a three dimensional structural model and the resulting changes in kinetics and soluble expression. The engineered phosphite dehydrogenase has great potential for NAD(P)H regeneration in industrial biocatalysis.

Keywords: Directed evolution, protein engineering, biocatalysis, NAD(P)H regeneration, cofactor regeneration, soluble expression.

INTRODUCTION

The use of enzymes for synthetic reactions has increased markedly over the past few decades and is continuing to grow [1-8]. Enzymes are very clean catalysts which offer environmentally safe disposal, have high specificity with few side reactions, and operate in aqueous solvents, at neutral pH, and at ambient temperatures. Moreover, often multiple simultaneous biotransformations can be carried out in a single reaction vessel. However, several hurdles still exist in order to realize their full potential for industrial utilization including difficulties in producing large quantities of enzymes, implementing desired substrate selectivity or specificity, high development costs, and sometimes low activities. Protein engineering technologies, notably directed evolution, have been successfully used to address many of these problems, leading to new enzyme catalysts with increased production, enhanced activity, altered specificities, and improved stabilities [7,9-12]. Even with these advances some problems still persist, such as performing complex enzymatic reactions that often require some type of cofactor. Cofactors are typically expensive and difficult to prepare, making their industrial use not feasible. Thus about 65% of industrially used enzymes are hydrolytic in nature and perform rather simple chemistry not requiring cofactors [1]. The common solution to this problem is

cofactor regeneration, which allows catalytic amounts of cofactors to be recycled during a bioconversion. An effective regeneration method simplifies product isolation, prevents problems due to product inhibition by the cofactor, and can help drive a thermodynamically unfavorable reaction by coupling it to a favorable regenerative reaction [13-16]. Enzymatic regenerative strategies have several distinct advantages over their electrochemical, chemical, biological, and photochemical counterparts that include high selectivity, compatibility with production enzymes, and high turnover rates in certain instances [13,15].

Nicotinamide cofactors are of special interest for regeneration since they are involved in nearly all physiological reductive processes, either directly, as in the case of NAD(P)H dependent dehydrogenases, or indirectly, as in many oxygenases where NAD(P)H is used to regenerate the reduced form of the enzyme. As such they are required for a number of industrially interesting reactions such as production of unnatural amino acids, polyols, and chiral alcohols [17,18]. This interest has led to the investigation of various chemical, electrochemical, and enzymatic methods for NAD(P)H regeneration [14,16,19], with the current state of the art being the formate/formate dehydrogenase system [20] as used on the preparative scale by Degussa for production of *L-tert*-leucine [21,22]. Recently, we have investigated phosphite dehydrogenase from *Pseudomonas stutzeri* as a suitable alternative to this system [23-25]. Phosphite dehydrogenase catalyzes the nearly irreversible oxidation of phosphite to phosphate and concomitant reduction of NAD to NADH [26]. Furthermore, a mutant enzyme has been developed that can successfully reduce both NAD and the significantly more expensive NADP with high

*Address correspondence to this author at the Departments of Chemistry and Chemical and Biomolecular Engineering, University of Illinois at Urbana-Champaign, 600 S. Mathews Ave, Urbana, IL 61801, USA; Tel: (217) 244-5360; Fax: (217) 244-8024; E-mail: vdonk@uiuc.edu and Tel: (217) 333-2631; Fax: (217) 333-5052; E-mail: zhao5@uiuc.edu

efficiency [24]. Other benefits of this system include the simple preparation of labeled phosphite from D₂O or T₂O [27], which can then be used to produce specifically labeled fine chemicals [25].

The primary cost for regenerative biocatalytic processes besides cofactors resides in the biocatalysts themselves. Therefore, in order to make a process economically viable, the regenerative enzyme must be relatively inexpensive in terms of cost per unit, making optimization of enzyme production extremely important. WT PTDH can be heterologously expressed in reasonable yields in *E. coli* [24,26], but improved expression levels would have important economic benefits. In addition, while the turnover rate for WT PTDH is comparable or better than the various forms of FDH [28,29], the large free energy of the PTDH catalyzed reaction ($\Delta G^{\circ} = -63.3$ kJ/mol) suggests that the turnover rate could be enhanced. In this work, directed evolution was utilized to improve the catalytic activity and soluble expression level of PTDH. A two tiered screening and selection method based on PTDH activity was developed and used in combination with error prone-PCR (EP-PCR). Following six rounds of mutagenesis and sorting, a significantly improved PTDH for NAD(P)H regeneration has been engineered.

EXPERIMENTAL SECTION

Materials. *E. coli* BW25141 [30,31] were a generous gift from Professor William Metcalf. The *phoBR(-)* phenotype of this strain prevents phosphate starvation response [32], *ΔaraBAD* prevents arabinose metabolization, and the integrated *pir* gene allows replication of *pir* dependent plasmids. The plasmid pRW2 was created as previously described [24] from pLA2 [33] containing a *pir* dependent replication origin that allowed it to be replicated in low copy number in cells containing the *pir* gene and it utilizes an arabinose promoter making it ideally suited for use with *E. coli* BW25141. *E. coli* BL21 (DE3), pET15b and pET26b(+) were all purchased from Novagen (Madison, WI). Nitro blue tetrazolium (NBT), phenazine methosulfate (PMS), ampicillin, kanamycin, *L-tert-leucine*, β-D-thiogalactopyranoside (IPTG), NAD and NADP were purchased from Sigma (St. Louis, MO). Restriction enzymes and T4 DNA ligase were purchased from New England Biolabs (Beverly, MA). Cloned *PfuTurbo* DNA polymerase was obtained from Stratagene (La Jolla, CA) while *Taq* polymerase was obtained from Promega (Madison, WI). Sodium phosphite was obtained from Riedel de Haen (Seelze, Germany), ammonium phosphite from City Chemicals (West Haven, CT), and phosphorous acid from Aldrich (St. Louis, MO). Kits for plasmid purification, gel and PCR purification of DNA were obtained from Qiagen (Valencia, CA). DNA oligonucleotide primers were obtained from Integrated DNA technologies (Coralville, IA). Trimethylpyruvic acid (85%) was generously donated by Carus Chemical Company (Lasalle, IL) and was then precipitated by neutralization with ammonia, and subsequently recrystallized by dissolving in minimal water and adding acetone:diethyl ether (5:1). Crystals were collected and washed with diethyl ether using vacuum filtration and dried overnight. Leucine dehydrogenase was purchased from Jülich Fine Chemicals (Jülich, Germany).

Mutagenesis and Library Construction. In all rounds except round 4, genetic diversity was created by error-prone PCR. The fidelity of *Taq* polymerase was modified by unbalanced dNTP concentrations in the presence of Mn²⁺ [34]. The PTDH gene was amplified using pRW2 specific flanking primers forward (5'-TTT TTG GAT GGA GGA ATT CAT ATG-3', *NdeI* restriction site is underlined) and reverse (5'-CGG GAA GAC GTA CGG GGT ATA CAT GT-3', *PciI* restriction site is underlined). In round 2, a saturation mutagenesis reverse primer was used (5'-CGT ACG GGG TAT ACA TGT TTA TCN VNN TGC GGC AGG VNN GGC CTT GGG C-3' V=A,C,G, *PciI* restriction site is underlined and degenerate regions in bold) to add additional diversity to the C-terminus of PTDH. A typical error-prone PCR reaction mixture contained 50 ng of pRW2 plasmid template, 1 x Promega *Taq* buffer, 7 mM MgCl₂, 0.15 MnCl₂, 0.2 mM each dATP and dGTP, 1 mM each dCTP and dTTP, 0.5 μM of each primer and 5 units of *Taq* DNA polymerase (Promega) in a 100 μL reaction volume. The reaction was cycled 20 times through typical melting, annealing and extension temperatures of 95, 55, and 72 °C respectively. In the 4th round the E175A mutation was introduced by site directed mutagenesis using the method described previously [24]. The PCR products were purified using a QIAquick PCR purification kit (Qiagen) and digested with *PciI*, *NdeI*, and *DpnI*. The resulting products were purified again, and ligated with *NdeI* and *PciI* digested pRW2. Following overnight ligation at 16 °C, the 10 μL reactions containing ~150 ng of DNA were precipitated by addition of 50 μL water and 500 μL 1-butanol and resuspended in 10 μL water.

Selection and Screening. Aliquots of electrocompetent *E. coli* BW25141 (50 μL) were transformed with 2.5 μL of the ligated library DNA. These cells were recovered in SOC media for 45 min with shaking at 250 rpm, centrifuged at 1000 x g, and washed with 1 mL of water and resuspended to a final volume of 100 μL. A small portion of these cells was plated on LB + kanamycin (50 μg/mL) solid media to check library size and the remainder was plated on solid PTDH selection media. The library sizes ranged from 2 x 10⁵ to 2 x 10⁶ clones. Solid PTDH selection media consisted of 15 g of agarose which was washed several times to remove residual phosphate and autoclaved in 1 L millipure water. This served as the base for 0.4% glucose-MOPS minimal media lacking phosphate to which varying concentrations of phosphite (0.5-250 mM) and arabinose (0.5-10 mM) were added for selection. After 60 hours growth at 37 °C, individual colonies were picked from the PTDH selective solid media and grown in 96 well plates in liquid LB plus kanamycin. The clones were then subjected to a secondary screen based on the rate of NBT reduction as previously described [24]. The most active clones in the NBT assay were selected, grown and induced in 5 mL LB media plus 50 μg/mL kanamycin, lysed, and reassayed by the NBT method. The best mutants at the end of each round served as the templates for the next round of mutagenesis.

Mutant Analysis. PTDH genes from the most active clones of each round were sequenced at the Biotechnology Center of the University of Illinois using the Big Dye™ Terminator sequencing method and an ABI PRISM® 3700 sequencer (Applied Biosystems, Foster City, CA). To accurately determine the fold improvement of the best

mutant for each round, lysates prepared as above were assayed in 10 mM NAD, 10 mM phosphite, and 50 mM MOPS buffer, pH 7.25 by measuring the increase in absorbance at 340 nm corresponding to production of NADH. These lysates were also analyzed by SDS-PAGE [35] followed by Coomassie blue staining and densitometry analysis using a Bio-Rad Gel-Doc with Quantity One software to determine the relative expression of the mutant PTDH enzymes. Only protein bands on the same gel were compared and this experiment was repeated in triplicate to obtain accurate results. The genes of the best mutants were subcloned into pET15b as previously described [24]. These constructs were then used to transform BL21 DE3 (Novagen), which were used to overexpress the encoded His₆-tagged PTDH proteins that were purified by immobilized metal affinity chromatography (IMAC) as previously described [24]. Protein concentration was determined by Bradford assay and by using the experimentally determined extinction coefficient of 30 mM⁻¹ cm⁻¹. Mutations were visualized *in silico* utilizing the previously created homology model [44]. The mutations were incorporated into this model using the rotamer explorer operation in Molecular Operating Environment followed by energy minimization using the MMF94s forcefield.

Steady-state Kinetic Measurements. Kinetic measurements were taken and substrate concentrations were measured as previously described [24]. At least 6 concentrations of each substrate were used varying from below the K_M value to at least 5-times higher than the K_M value while the other substrate was kept at a constant saturating concentration. The Michaelis-Menton equation was fitted to the data using non-linear least squares regression analysis in Origin 5.0 to determine *k*_{cat} and K_M values. To determine the primary kinetic isotope effect on *k*_{cat}, deuterated phosphite was prepared as described elsewhere [27] and the activity was measured with saturating concentrations of NAD (5 mM) and labeled or unlabeled phosphite (20 mM).

Fermentation. Non-His₆-tagged constructs were created by ligating a *Nde*I and *Bam*HI digested WT and round 6 PTDH gene into a similarly prepared pET26b vector. These vectors were used to transform BL21 (DE3) and their sequences were confirmed by automated DNA sequencing. Fermentation was carried out at the Ohio State University's Fermentation Facility. Briefly, a starter culture was grown overnight in terrific broth plus kanamycin and transferred to the fermentor containing 10 L of terrific broth with kanamycin. The cells were grown to an OD₆₀₀ of 0.6 and cooled to 25 °C at which time induction of protein expression was started with the addition of 0.5 mM IPTG. After 8 hours of protein expression the cells were collected by centrifugation, weighed, and frozen at -80 °C. Equal amounts of cell lysate prepared by treatment with lysozyme and sonication were analyzed to determine PTDH activity as described in the kinetic measurements section.

Production of L-tert-Leucine. Small-scale regeneration reactions containing 100 mM ammonium trimethylpyruvate, 200 mM diammonium phosphite, 0.4 mM NAD, 5.26 U/mL of leucine DH, and 57.5 µg/mL WT PTDH (0.265 U/mL) or round 6 PTDH (0.508 U/mL). The reactions were mixed gently and incubated at 25 °C. At fixed time

intervals, samples were removed from the reaction and immediately frozen at -80 °C. The frozen samples were thawed immediately prior to HPLC analysis. A Shimadzu HPLC equipped with an evaporative light scattering detector was used to quantify the amount of *tert*-leucine in each sample following separation on a Alltech C-18 prevail column with an isocratic elution of 94% water, 5% acetonitrile, and 1% acetic acid. The peak area of *tert*-leucine in each sample was converted to concentration by a standard curve prepared with five known concentrations of authentic *L*-*tert*-leucine. The steady state rates for the reactions were determined by fitting the first four data points to a line by linear regression analysis.

RESULTS AND DISCUSSION

Selection and screening method. A two tiered selection and screening method for enhancing the activity of phosphite dehydrogenase was developed. There was a previously established method for selecting *E. coli* which have the ability to produce their own phosphate from various reduced phosphorus compounds [36]. We mimicked this type of selection using phosphate free glucose-MOPS minimal media containing 0.5 mM phosphite and *E. coli* BW25141, which lack the ability to activate phosphate starvation pathways. Using this selection, we could distinguish between *E. coli* BW25141 heterologously expressing PTDH and those that were not. However, distinguishing between different levels of PTDH activity required some optimization. PTDH was cloned into the expression vector pRW2 under the control of an arabinose promoter, and the threshold concentration of the inducer arabinose that gave the minimum PTDH expression which allowed growth of *E. coli* BW25141 was determined. The first round of selection was thus performed using arabinose concentrations (controlling PTDH expression levels) just below the determined threshold. This method, however, did not yield mutants with large increases in total enzymatic activity, but rather resulted in mutations that primarily decreased K_M values for phosphite as discussed below. To address this problem, the selection was altered for subsequent rounds based on phosphite's toxicity, which can inhibit many phosphate dependent pathways when present at a high enough concentration. The rationale for the change in selection method was that *k*_{cat} would be more likely to improve at high concentrations of phosphite, whereas K_M improvements seen in the first round resulted from low intracellular phosphite concentrations. Thus, the maximum phosphite concentration threshold that *E. coli* BW25141 expressing the first round PTDH mutant could still survive on was determined (Fig. 1A). Concentrations of phosphite above this threshold were utilized to select for mutants with higher activity during subsequent rounds of sorting. After each round a new maximum phosphite concentration threshold was established. Any *E. coli* BW25141 cells without sufficient PTDH activity to convert the toxic level of phosphite to a non-toxic level should not survive the selection. This selection method was successfully used in rounds 2-6 and the concentration of phosphite at which the mutants could grow increased from 50 mM in round 2 to 250 mM in the final round. Each of the successive best mutants for the 6 rounds of directed evolution displayed a gradual increase in concentration of phosphite required to

inhibit cell growth, which corresponded to a gradual increase in total activity of the cell lysate as assessed with a coupled NBT assay that reports on the amounts of NADH produced (Fig. 1B) [24].

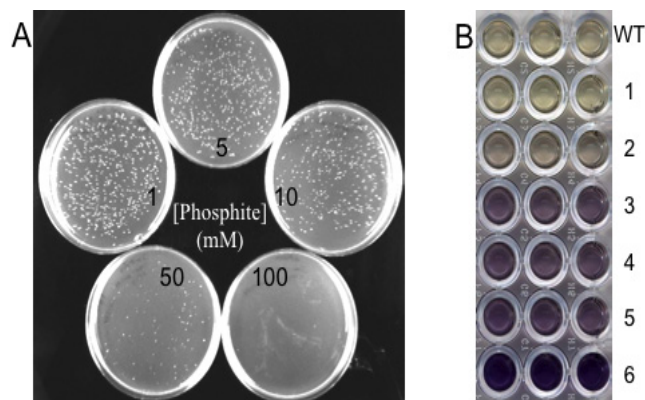


Fig. (1). A) Example of a selection based on phosphite toxicity using increasing phosphite concentrations. Minimal media plates containing 1, 5, 10, 50, or 100 mM phosphite have different levels of growth of *E. coli* BW25141 transformed with the pRW2-Round3 mutant library. Subsequently, 100 mM phosphite was chosen as the concentration for the third round selection. B) Result of an NBT assay comparing the lysates from the best mutants in each round ten minutes after adding the components of the NBT coupled assay [24].

Amino Acid Substitutions. The amino acid substitutions for the best mutants of each round are listed in Table 1. In round 1, many proteins of similar total activity had mutations clustered near the C-terminus at positions 332, 336, and 337 (one of two stop codons) in addition to K330 being changed to a stop codon (K330*). To investigate the effect of sequence alterations at the C-terminus in more detail, in round 2, EP-PCR was coupled to saturation mutagenesis at codons 332, 336 and 337. The variant protein with the highest total activity had two mutations (E332N and C336D) from saturation mutagenesis and one mutation (M26I) from EP-PCR. This enzyme had better total activity than the K330* mutant of round 1 and was therefore carried on as the parent for EP-PCR in round 3, which revealed D13E as an important mutation. Site-directed mutagenesis was utilized in round 4 to incorporate the E175A mutation previously shown to allow NADP utilization and increase the turnover rate [24]. The libraries used in rounds 5 and 6 were generated by EP-PCR and the mutations T181S and A308T were found, respectively.

Total Activity and Soluble Expression Enhancement. One drawback to the cell lysate assay is that only total activity can be determined and therefore it is unclear what parameters (i.e. expression level, solubility or kinetics) have caused the increase in total enzymatic activity. Therefore, the best mutant from each round was characterized in greater detail to dissect the contributions to the improvements. First, in order to assign an accurate numeric improvement in total activity, lysates were assayed by analyzing production of NADH at 340 nm in the presence of saturating concentrations of phosphite and NAD. In addition, to determine the role played by enhanced soluble expression in the increased activity, SDS-PAGE and densitometry were

utilized. Fig. 2A shows the average increase in relative total activity for each of the mutants (white bars) next to the average relative amounts of soluble PTDH (grey bars) showing an approximate 6.2-fold improvement in the total activity of the final mutant over the WT enzyme with the largest increases in the first three rounds. The first round mutant only had a small enhancement in total activity, mostly as a result of increased expression level and not of enhanced catalytic activity, prompting the change in selection methodology mentioned above. Using the method that selects for higher phosphite detoxification rates, the next two rounds of directed evolution resulted in the greatest enhancement in soluble expression and total activity, which were raised 2.7-fold and 4.8-fold, respectively, over the WT PTDH. The level of soluble expression was improved approximately 3.4-fold over the six rounds of directed evolution; about 2-fold less than the total activity enhancement. This difference between the enhancement in

Table 1. Mutations Discovered by Directed Evolution

Round	Amino Acid Change	Codon Change
WT	None	None
1	K330*	AAG to TAG
2 ^a	M26I	ATG to ATA
	E332N	GAG to AAT
	C336D	TGT to GAC
3	D13E	GAA to GAT
	M26I	ATG to ATA
	E332N	GAG to AAT
	C336D	TGT to GAC
4 ^b	D13E	GAA to GAT
	M26I	ATG to ATA
	E175A	GAG to GCG
	E332N	GAG to AAT
	C336D	TGT to GAC
5	D13E	GAA to GAT
	M26I	ATG to ATA
	E175A	GAG to GCG
	T181S	ACA to TCA
	E332N	GAG to AAT
	C336D	TGT to GAC
6	D13E	GAA to GAT
	M26I	ATG to ATA
	E175A	GAG to GCG
	T181S	ACA to TCA
	A308T	GCA to ACA
	E332N	GAG to AAT
	C336D	TGT to GAC

^aRound 2 mutant was created by EP-PCR coupled to saturation mutagenesis of WT at positions 332, 336, and 337. ^bRound 4 mutant was created by site-directed mutagenesis. *stop codon.

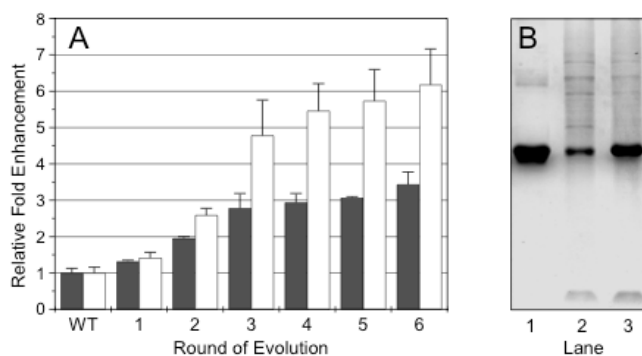


Fig. (2). A) Comparison of the total lysate activity (white bars) and soluble expression (gray bars) for the best mutant from each round. The final mutant has >6-fold improvement in total activity and >3-fold improvement in soluble expression levels. B) SDS-PAGE analysis of PTDH expressed in BL21 (DE3) as a His₆-Tag fusion. Lane 1 contains WT PTDH purified by IMAC and is shown as a standard, lane 2 contains the soluble lysate fraction of BL21 (DE3) pET15b- WT PTDH post expression, and lane 3 contains the soluble lysate fraction of BL21 (DE3) pET15b-Round 6 PTDH mutant post expression. There is approximately 3-fold more soluble PTDH expression in lane 3 than in lane 2.

expression and total activity suggests that in addition to enhanced expression, the turnover rate was also improved. To test this hypothesis, the mutant enzymes were expressed as His₆-tag fusions and purified by IMAC. The soluble overexpression of these constructs was also analyzed by SDS-PAGE and densitometry to verify that the improvement in total activity was not strain or vector dependent, but rather

PTDH sequence dependent. Fig. 2B shows the clear difference in the overexpression levels of the His₆-WT PTDH in comparison to the His₆-tagged mutant from round 6, which maintained the 3-fold difference in BL21(DE3) that was previously found with expression from pRW2 in *E. coli* BW25141. Therefore, the expression improvement was not vector or *E. coli* strain dependent and resulted in excellent production of the final mutant PTDH.

Kinetics of Purified Mutant PTDHs. The kinetic parameters of each purified enzyme were determined as described in Materials and Methods and are listed with NAD as the cofactor at the top of Table 2. The k_{cat} of the best mutant of round 1 was not significantly altered, which is in good agreement with Fig. 2A, suggesting that the enhancement comes from increased soluble expression. However, in rounds 2-6 a gradual increase in k_{cat} was obtained with a 2-fold higher turnover rate for the final mutant over that of the WT PTDH, which also agrees with the lysate data (Fig. 2A). Overall, the round 1 mutant had lower K_M values for both substrates, while the incorporation of the E175A mutation in round 4 caused the K_M values for both phosphite and NAD to increase. The final mutant had K_M values that were essentially unchanged from those of the WT enzyme, resulting in catalytic efficiencies that were 2-fold better for both substrates.

The kinetic parameters were also determined with NADP as the cofactor and are presented in Table 2 (bottom) along with those of the isolated E175A mutation in WT-PTDH that was previously characterized [24]. With NADP the k_{cat} is also enhanced in the mutants, however, to a lesser degree than just the E175A mutation. As expected, a major decrease

Table 2. Kinetic Parameters for Phosphite Dehydrogenase Mutants with NAD(P)

NAD					
Enzyme	k_{cat} (min ⁻¹)	K_M, NAD (μM)	$k_{cat}/K_M, NAD$ (μM ⁻¹ min ⁻¹)	K_M, Pt (μM)	$k_{cat}/K_M, Pt$ (μM ⁻¹ min ⁻¹)
WT	176 ± 8	53 ± 9	3.3	47 ± 6	3.7
Rnd 1	168 ± 6	37 ± 5	4.5	14 ± 3	12
Rnd 2	217 ± 9	32 ± 3	6.8	27 ± 2	6.8
Rnd 3	220 ± 20	34 ± 8	6.5	30 ± 1	7.3
Rnd 4	240 ± 20	41 ± 6	5.9	82 ± 2	2.9
Rnd 5	260 ± 5	39 ± 1	6.7	84 ± 2	3.1
Rnd 6	340 ± 30	45 ± 1	7.6	48 ± 2	7.1
NADP					
Enzyme	k_{cat} (min ⁻¹)	$K_M, NADP$ (μM)	$k_{cat}/K_M, NADP$ (μM ⁻¹ min ⁻¹)	K_M, Pt (μM)	$k_{cat}/K_M, Pt$ (μM ⁻¹ min ⁻¹)
WT	85 ± 1	2500 ± 400	0.034	1900 ± 300	0.045
Rnd 3	105 ± 9	1070 ± 50	0.098	1900 ± 600	0.055
Rnd 4	110 ± 1	65 ± 8	1.7	87 ± 2	1.3
Rnd 5	112 ± 10	57 ± 9	2.0	62 ± 9	1.8
Rnd 6	114 ± 5	56 ± 5	2.0	70 ± 10	1.6
E175A	130 ± 0.4	140 ± 10	0.91	138 ± 25	0.94

All assays were performed at 25 °C pH 7.25 in 50 mM MOPS.

occurred in the K_M value for NADP upon incorporation of the E175A mutation in round 4, which also lowered the K_M for phosphite. This mutation seems to work synergistically with other mutations as the final mutant has K_M values that are approximately 2-fold lower than those obtained with the E175A mutation alone. The final mutant therefore has catalytic efficiencies for both NADP and phosphite (with NADP) that are nearly 2 orders of magnitude higher than WT PTDH.

The observed turnover rate enhancement with NAD of 2-fold is a significant improvement for protein engineering of a native activity. We initially anticipated that even greater improvements could be obtained based upon the large free energy of the PTDH catalyzed reaction ($\Delta G^\circ = -63.3$ kJ/mol) and its relatively low turnover rate in the native enzyme. However, no further improvements could be obtained by EP-PCR after the 2-fold increase in k_{cat} . Several other D-hydroxyacid dehydrogenases belonging to the same family as PTDH have much higher k_{cat} values in the same direction, such as D-lactate DH ($k_{cat} \approx 9,000 \text{ min}^{-1}$) [37] and glycerate DH ($k_{cat} \approx 2200 \text{ min}^{-1}$) [38]. However, PTDH and FDH (also a D-hydroxyacid DH) both utilize small substrates, have considerable thermodynamic driving forces (FDH $\Delta G^\circ = -33.2$ kJ/mol, PTDH $\Delta G^\circ = -63.3$ kJ/mol), and both have much lower turnover rates. This is not the result of a slow physical step limiting the rate of catalysis since for FDH, hydride transfer is completely rate limiting [39] and for PTDH, hydride transfer is at least partially if not fully rate determining [27]. One possible explanation for the comparatively low activity of PTDH features a reverse protonation type mechanism [40,41]. Although this postulate remains to be experimentally tested, if this is the case then it would be difficult to further increase the catalytic efficiency of the enzyme considerably.

The improvements in k_{cat} render PTDH very competitive in terms of turnover rate with the three most commonly used FDH enzymes from *Candida boidinii*, *C. methylca*, and an NADP specific mutant from *Pseudomonas sp.101*, which have k_{cat} values of 240 min^{-1} [42], 84 min^{-1} [43], and 300 min^{-1} [29], respectively, with NAD as the cofactor. The final PTDH mutant has a higher k_{cat} value (340 min^{-1}) than the above-mentioned FDH enzymes. Additionally, at 25°C where regenerative enzymatic reactions are preferentially carried out and PTDH was assayed, the FDH turnover rates will be significantly lower than at 30°C where they were measured. The K_M value for the sacrificial substrate is also much lower for the final PTDH mutant ($48 \mu\text{M}$ phosphite) than for any of these FDH enzymes ($5\text{--}9 \text{ mM}$ formate) [28,29,42,43]. Thus, the catalytic efficiency (k_{cat}/K_M) in terms of the sacrificial substrate for the final PTDH mutant is >150 -fold higher than any of the FDH enzymes. As for NADPH regeneration, the k_{cat} for the final PTDH mutant is comparable at 114 min^{-1} to the NADP specific mutant FDH from *Pseudomonas* (150 min^{-1}), but K_M values of the PTDH mutant are significantly lower for both NADP and the sacrificial substrate. Therefore, in terms of turnover rate and catalytic efficiency for regenerative processes the final PTDH mutant appears to be superior to commonly utilized FDH enzymes. In the future, an enzymatic membrane reactor will be utilized to appropriately compare process productivities and economics of the FDH and PTDH cofactor regeneration systems.

Kinetic Isotope Effect. Saturating concentrations of NAD and deuterated phosphite were utilized to determine a primary kinetic isotope effect on k_{cat} of 2.1 ± 0.1 for the final mutant, which is the same as the previously reported isotope effect for WT PTDH [27]. Therefore, hydride transfer is rate limiting to the same degree in the final mutant as with the WT enzyme, suggesting no major change in the isotope sensitive step or in steps that may mask the overall isotope effect. An additional advantage of using PTDH as a NAD(P)H regeneration biocatalyst is that deuterium (or tritium) labeled products can be produced with only this modest reduction in turnover rate and from deuterated phosphite, which is cheap and easy to produce from D_2O and phosphorous acid [27].

Enzyme Production. In order to determine the maximum yield of the final PTDH mutant in comparison to the WT PTDH, non His₆-tagged overexpression constructs based on pET26b(+) were prepared and transformed into BL21(DE3). The cells were then grown and induced using a 10 L batch fermentor followed by cell lysis as described in the Experimental Section. *E. coli* BL21(DE3) cells harboring the round 6 PTDH mutant grew to a higher overall density, yielding 26% more cell wet mass (101 g) than those harboring WT PTDH (80 g). The total activity of the lysates for the WT was $\sim 70 \text{ U/g}$ wet cell mass (600 U/L fermentation), while for the round 6 enzyme it was improved to $\sim 360 \text{ U/g}$ wet cell mass (3700 U/L fermentation). This represents a ~ 5 -fold (6-fold by volume) improvement of the mutant over the WT, which corresponds well to the total lysate activity improvement in Fig. 2A with pRW2 in *E. coli* BW25141. Furthermore, while this process still stands to gain considerably from process optimization, its productivity compares well to some fully optimized processes for producing FDH [29].

Regeneration of NADH for L-tert-Leucine Production. Production of L-tert-leucine from trimethylpyruvate is an ongoing industrial transformation carried out by Degussa, which utilizes the formate/FDH regeneration system to regenerate the reduced cofactor [21]. As shown in Fig. 3, the phosphite/PTDH system also has potential for this transformation. The WT PTDH and final PTDH mutant were probed for cofactor regeneration by coupling them with leucine dehydrogenase (LeuDH) for the production of L-tert-leucine. In this scheme (Fig. 3A), PTDH converts NAD to NADH during conversion of phosphite to phosphate, which doubles as the buffer. The produced NADH is utilized by LeuDH to convert trimethylpyruvate and ammonia to L-tert-leucine. This reaction was performed under conditions in which the conversion of NAD to NADH by PTDH was limiting for the overall rate of the reaction. When equal molar amounts of WT PTDH and the round 6 mutant PTDH were used in separate reactions, the reactions proceeded much faster with the mutant, which reached completion nearly twice as fast as the reaction with the WT enzyme. The reaction rate at the linear portion of the reaction was determined using the first four data points of L-tert-leucine production for each enzyme. The reaction rate of the WT enzyme in this linear region was $\sim 11 \text{ mM/hour}$, whereas the reaction rate of the final mutant was about twice as fast at $\sim 22 \text{ mM/hour}$, correlating well to the difference in their determined k_{cat} values.

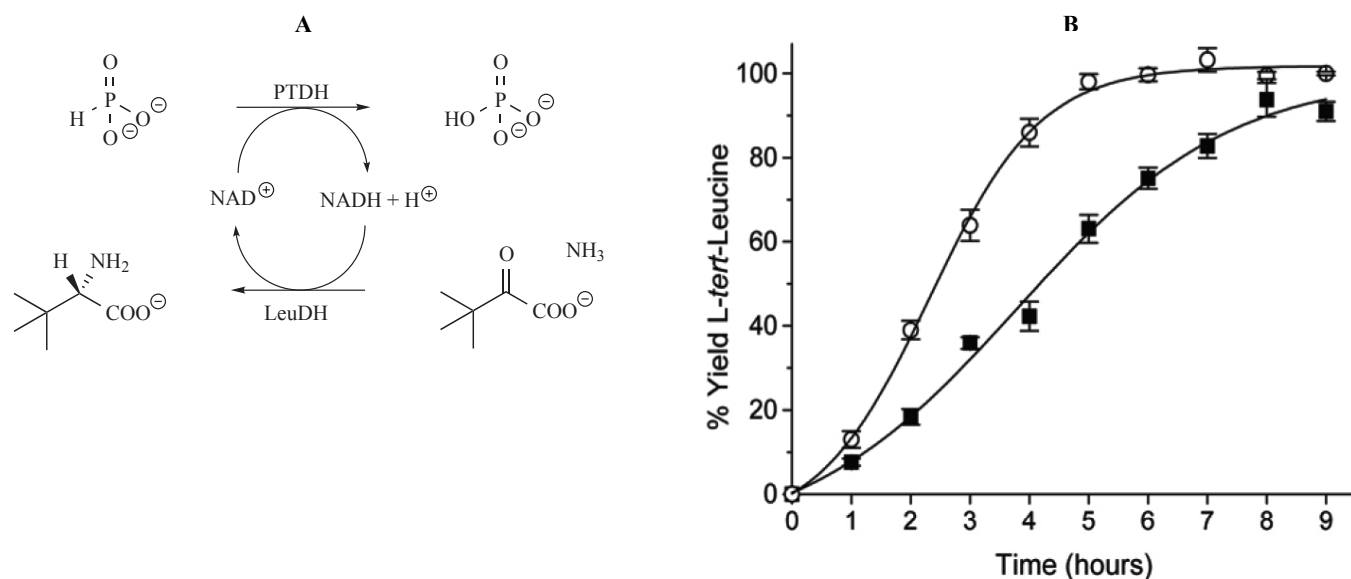


Fig. (3). A) Scheme for production of *L*-*tert*-leucine from trimethylpyruvate and ammonia by leucine dehydrogenase with NADH regeneration by the phosphite/PTDH system. B) Comparison of equal amounts (by mass) of WT-PTDH (■) and round 6 mutant PTDH (○) for NADH regeneration in the production of *L*-*tert*-leucine. Production of *L*-*tert*-leucine was measured at the various time points by HPLC.

Structural and Functional Analysis of Mutations. Fig. 4 displays a homology model of PTDH [24] with the locations of the seven mutations (in red) in relation to a bound NAD molecule and the catalytic residues (in green). Upon inspecting this structural model, it is immediately evident that none of the mutations is near the three proposed catalytic residues [40]. The closest mutation is E332N, which is still over 9 Å away from the nearest catalytic residue (R237). Several mutated residues are near the NAD cofactor-binding pocket including N332, D336, and A175. It has become a common theme in directed evolution to find mutations that are far from the catalytic center of an enzyme, yet affect enzymatic activity [44-47].

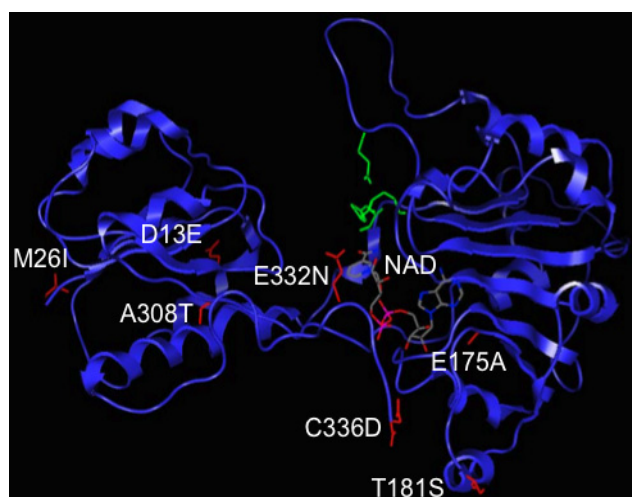


Fig. (4). Homology model of the round 6 mutant. Mutated residues are labeled in white font and shown in red as sticks, while the proposed catalytic residues (His 292, Arg 237, and Glu 266) are shown in green as sticks. NAD is colored by atom type. All of the mutated residues are greater than 9 Å away from the catalytic residues, although several may interact with the bound cofactor.

In the first round, the preponderance of mutations were found near the C-terminus of the protein, with the best performing mutant lacking the last seven residues resulting in reduced K_M values (Table 1) and slightly enhanced expression. This suggests that the C-terminal region of the protein interferes with substrate binding, a hypothesis that is supported by the homology model in which the C-terminus appears to cap the NAD binding site (Fig. 4). Previously, the C-terminal cysteine was proposed to have a possible regulatory role [24] in an analogous fashion to malate DH where disulfide bond formation involving the C-terminal Cys blocks NADP binding [48,49]. Here, mutations that remove or change this residue in PTDH result in higher activity, which may be related to eliminating disulfide bond formation.

Saturation mutagenesis of the C-terminal region in the second round resulted in E332N and C336D combined with the M26I mutation from error-prone PCR as the best overall variant. This mutant exhibited a slightly higher turnover rate, mostly as a result of the removal of the C-terminal cysteine, possibly coupled to minor shifts in NAD binding due to contacts of the new N332 and D336 residues. The additional enhanced soluble expression of this mutant likely results from the M26I mutation, which is distant from the active site (~35 Å) and appears to be solvent exposed. Since the mutation itself does not greatly change the hydrophilicity of this residue, packing factors may be more important for the resulting improved soluble expression level. The D13E mutant found in the third round is also solvent exposed, far from the active site, and is a rather conservative mutation that results in increased expression level without large changes in k_{cat} (Table 2). E175A was incorporated in the fourth round and opens the pocket where the adenine ribose phosphate of NADP would bind [24], allowing this mutant to utilize both NAD and NADP efficiently (Table 2). This mutation was previously characterized in more detail with the WT PTDH enzyme as a template [24] and here the effects

of this mutation are similar, except that the K_M values of NAD(P) for the round 4 enzyme are much smaller than for the previously reported E175A-WT PTDH (Table 2).

The final two mutations identified were T181S and A308T and again both are far from the active site. These two mutations affect predominantly the k_{cat} of the enzyme. It is possible that A308T causes a minor change in the folding or position of the α -helix where it is located, which subsequently alters the position of the proposed catalytic base H292 just upstream of that α -helix. It is not obvious why T181S would affect k_{cat} , as it is not close in sequence or location to any catalytic residues. Clearly, none of these mutations could have been predicted *a priori* besides the rationally incorporated E175A mutation and some of them are difficult to explain functionally, thus highlighting the power of combinatorial approaches such as directed evolution.

CONCLUSION

The phosphite oxidation activity of phosphite dehydrogenase from *Pseudomonas stutzeri* heterologously expressed in *E. coli* was successfully enhanced. Seven mutations were discovered that each contributed to enhanced total activity as a result of increased turnover rate and/or increased soluble expression. These improvements are significant in terms of industrial application since the primary cost of cofactor regeneration systems is the production cost of the enzymes. The production yield of the final mutant biocatalyst was successfully increased 6-fold compared to the WT enzyme, thus reducing the cost of a PTDH regenerative process by approximately the same amount. The mutant enzyme can be produced at the level of 360 U/g wet cells (*E. coli*), which compares well with FDH production yields [29]. The improvement of the final mutant was displayed for NADH regeneration in the industrially relevant production of *L-tert-leucine*. Furthermore, the longevity of PTDH has been improved by enhancing its thermal stability [23]. In ongoing studies, this process and others including the production of xylitol by xylose reductase and preparation of chiral alcohol building blocks by alcohol dehydrogenase are being optimized under membrane reactor conditions for the best space/time yield in order to compare them directly to productivity with the formate/FDH regeneration system. With the enhancements in expression and activity of PTDH described here, important steps have been taken towards the generation of a industrially viable NAD(P)H regeneration system.

ACKNOWLEDGEMENTS

Support for this research was provided by Biotechnology Research and Development Consortium (BRDC) (Project 2-4-121). Fermentations were carried out with the help of Ohio State University's Fermentation Facilities and staff. We thank Carus Chemical Company (LaSalle, IL) for generously donating a large sample of trimethylpyruvic acid.

REFERENCES

[1] Faber, K. *Biotransformations in Organic Chemistry*; 5th edition ed.; Springer Verlag: Berlin, Germany, 2004.
 [2] Zaks, A. *Curr. Opin. Chem. Biol.*, **2001**, *5*, 130-136.

[3] Schmid, A.; Dordick, J.S.; Hauer, B.; Kiener, A.; Wubbolts, M.; Witholt, B. *Nature*, **2001**, *409*, 258-268.
 [4] Liese, A.; Filho, M.V. *Curr. Opin. Biotechnol.*, **1999**, *10*, 595-603.
 [5] Koeller, K.M.; Wong, C.H. *Nature*, **2001**, *409*, 232-240.
 [6] Huisman, G.W.; Gray, D. *Curr. Opin. Biotech.*, **2002**, *13*, 352-358.
 [7] Kirk, O.; Borchert, T.V.; Fuglsang, C.C. *Curr. Opin. Biotech.*, **2002**, *13*, 345-351.
 [8] Wandrey, C.; Liese, A.; Kihumbu, D. *Org. Process. Res. Dev.*, **2000**, *4*, 286-290.
 [9] Zhao, H.; Chockalingam, K.; Chen, Z. *Curr. Opin. Biotechnol.*, **2002**, *13*, 104-110.
 [10] Woodyer, R.; Chen, W.; Zhao, H. *J. Chem. Educ.*, **2004**, *81*, 126-133.
 [11] Arnold, F.H.; Volkov, A.A. *Curr. Opin. Chem. Biol.*, **1999**, *3*, 54-59.
 [12] Schoemaker, H.E.; Mink, D.; Wubbolts, M.G. *Science*, **2003**, *299*, 1694-1697.
 [13] Zhao, H.; van der Donk, W.A. *Curr. Opin. Biotechnol.*, **2003**, *14*, 583-589.
 [14] Chenault, H.K.; Whitesides, G.M. *Appl. Biochem. Biotechnol.*, **1987**, *14*, 147-197.
 [15] Chenault, H.K.; Simon, E.S.; Whitesides, G.M. *Biotechnol. Genet. Eng. Rev.*, **1988**, *6*, 221-270.
 [16] Leonida, M.D. *Curr. Med. Chem.*, **2001**, *8*, 345-369.
 [17] Hummel, W.; Kula, M.R. *Eur. J. Biochem.*, **1989**, *184*, 1-13.
 [18] Krix, G.; Bommaris, A.S.; Drauz, K.; Kottenhahn, M.; Schwarm, M.; Kula, M.R. *J. Biotechnol.*, **1997**, *53*, 29-39.
 [19] van der Donk, W.A.; Zhao, H. *Curr. Opin. Biotechnol.*, **2003**, *14*, 421-426.
 [20] Kragl, U.; Kruse, W.; Hummel, W.; Wandrey, C. *Biotechnol. Bioeng.*, **1996**, *52*, 309-319.
 [21] McCoy, M. *Chem Eng News* **2001**, *79*, 37-43.
 [22] Woltinger, J.; Karau, A.; Leuchtenberger, W.; Drauz, K. *Adv. Biochem. Eng. Biotechnol.*, **2005**, *92*, 289-316.
 [23] Johannes, T.W.; Woodyer, R.D.; Zhao, H. *Applied and Environmental Microbiology*, **2005**, (in press).
 [24] Woodyer, R.; van der Donk, W.A.; Zhao, H. *Biochemistry*, **2003**, *42*, 11604-11614.
 [25] Vrtis, J.M.; White, A.K.; Metcalf, W.W.; van der Donk, W.A. *Angew. Chem. Int. Ed. Engl.*, **2002**, *41*, 3257-3259.
 [26] Costas, A.M.; White, A.K.; Metcalf, W.W. *J. Biol. Chem.*, **2001**, *276*, 17429-17436.
 [27] Vrtis, J.M.; White, A.K.; Metcalf, W.W.; van der Donk, W.A. *J. Am. Chem. Soc.*, **2001**, *123*, 2672-2673.
 [28] Serov, A.E.; Popova, A.S.; Fedorchuk, V.V.; Tishkov, V.I. *Biochem. J.*, **2002**, *367*, 841-847.
 [29] Tishkov, V.I.; Galkin, A.G.; Fedorchuk, V.V.; Savitsky, P.A.; Rojkova, A.M.; Gieren, H.; Kula, M.R. *Biotechnol. Bioeng.*, **1999**, *64*, 187-193.
 [30] Datsenko, K.A.; Wanner, B.L. *Proc. Natl. Acad. Sci. USA*, **2000**, *97*, 6640-6645.
 [31] Lessard, I.A.; Pratt, S.D.; McCafferty, D.G.; Bussiere, D.E.; Hutchins, C.; Wanner, B.L.; Katz, L.; Walsh, C.T. *Chem. Biol.*, **1998**, *5*, 489-504.
 [32] Wanner, B.L. *J. Mol. Biol.* **1983**, *166*, 283-308.
 [33] Haldimann, A.; Wanner, B.L. *J. Bacteriol.*, **2001**, *183*, 6384-6393.
 [34] Fromant, M.; Blanquet, S.; Plateau, P. *Anal. Biochem.*, **1995**, *224*, 347-353.
 [35] Laemmli, U.K. *Nature*, **1970**, *227*, 680-685.
 [36] White, A.K.; Metcalf, W.W. *J. Bacteriol.*, **2004**, *186*, 5876-5882.
 [37] Kochhar, S.; Chuard, N.; Hottinger, H. *J. Biol. Chem.*, **1992**, *267*, 20298-20301.
 [38] Ali, V.; Shigeta, Y.; Nozaki, T. *Biochem. J.*, **2003**, *375*, 729-736.
 [39] Blanchard, J.S.; Cleland, W.W. *Biochemistry*, **1980**, *19*, 3543-3550.
 [40] Relyea, H.A.; van der Donk, W.A. *Bioorg. Chem.*, **2005**, *33*, 171-189.
 [41] Relyea, H.A.; Vrtis, J.M.; Woodyer, R.; Rimkus, S.A.; van der Donk, W.A. *Biochemistry*, **2005**, *44*, 6640-6649.
 [42] Slusarczyk, H.; Felber, S.; Kula, M.R.; Pohl, M. *Eur. J. Biochem.*, **2000**, *267*, 1280-1289.
 [43] Gul-Karaguler, N.; Sessions, R.B.; Clarke, A.R.; Holbrook, J.J. *Biotechnol. Lett.*, **2001**, *23*, 283-287.
 [44] Kim, D.; Guengerich, F.P. *Biochemistry*, **2004**, *43*, 981-988.
 [45] Horsman, G.P.; Liu, A.M.; Henke, E.; Bornscheuer, U.T.; Kazlauskas, R.J. *Chemistry*, **2003**, *9*, 1933-1939.

- [46] Spiller, B.; Gershenson, A.; Arnold, F.H.; Stevens, R.C. *Proc. Natl. Acad. Sci. USA*, **1999**, *96*, 12305-12310.
- [47] Liebeton, K.; Zonta, A.; Schimossek, K.; Nardini, M.; Lang, D.; Dijkstra, B.W.; Reetz, M.T.; Jaeger, K.E. *Chem. Biol.*, **2000**, *7*, 709-718.
- [48] Issakidis, E.; Saarinen, M.; Decottignies, P.; Jacquot, J.P.; Cretin, C.; Gadal, P.; Miginiac-Maslow, M. *J. Biol. Chem.*, **1994**, *269*, 3511-3517.
- [49] Krimm, I.; Goyer, A.; Issakidis-Bourguet, E.; Miginiac-Maslow, M.; Lancelin, J.M. *J. Biol. Chem.*, **1999**, *274*, 34539-34542.

Received: March 21, 2005

Revised: June 20, 2005

Accepted: June 20, 2005